Industrial Engineering
2026, Vol. 10, No. 2, pp. 49–62
https://doi.org/10.11648/j.ie.20261002.12

Research Article

Effect of Sliding Speed, Load, and Lubricant Viscosity on the Friction Behaviour of Soft Porous Lubrication

Duc Hieu Nguyen*

Faculty of Engineering Mechanics and Automation, VNU University of Engineering and Technology, Hanoi, Vietnam

Abstract

This study examines how sliding speed, applied load, and lubricant viscosity govern the friction behaviour of soft porous materials under dynamically evolving compression. Soft porous lubrication can generate load support while reducing friction by combining solid-matrix deformation with pore fluid pressurisation, but most existing theoretical models assume fixed compression and cannot capture the coupled response of real bearing systems. To address this gap, a modified Mini Traction Machine (MTM) was used, in which a cone-shaped upper specimen was paired with interchangeable soft porous samples on the lower disc, allowing the porous layer to compress and recover freely during operation rather than being held at a fixed thickness. Six porous materials — four open-cell polyurethane foams and two woven fibrous substrates, spanning a range of thicknesses and pore sizes — were tested dry and under water, glycerol (5% and 10%), and PEG 400 lubrication, across sliding speeds of 5-120 mm/s at constant load and normal loads of 1-7 N at constant speed. Dry friction coefficients ranged from approximately 0.1 (thin woven material) to 0.65 (thick open-pore foam), and results show that, contrary to predictions from steady-state, fixed-compression theory, friction did not consistently decrease with increasing sliding speed or applied load; for most materials the friction coefficient changed only marginally or even increased, indicating a self-regulating feedback loop in which rising pore pressure increases fluid lift, which in turn reduces compression and limits further pressure build-up. Introducing a liquid lubricant markedly reduced friction relative to dry contact, cutting the friction coefficient of the thinnest woven material from roughly 0.10 (dry) to as low as 0.02 with PEG 400 lubrication — a reduction of approximately 80% — although the benefit of increasing glycerol concentration plateaued beyond 5%. These findings demonstrate the limitations of fixed-compression theoretical models for soft porous lubrication and highlight the need for dynamic, compression-free testing protocols when selecting lubricant formulations and operating conditions for advanced low-friction, long-life bearing designs.

Keywords

Friction, XPHD, Soft Porous Media, Lubrication, Sliding Speed, Fluid Viscosity, Mini Traction Machine, Bearing Design

1. Introduction

The study of friction in the context of soft porous lubrication, so-called Ex-Poro-Hydrodynamic (XPHD), is crucial for advancing the design of future bearing systems that exploit this mechanism. A major advantage of soft porous lubrication lies in its ability to generate load support while reducing friction, leveraging both the solid and fluid phases of the porous material in contact with sliding surfaces, both at low and large speeds [1]. In this biphasic system, pore fluid pressure and

*Correspondence: Duc Hieu Nguyen (ndhieu@vnu.edu.vn)

Received: 12 August 2026; **Accepted:** 24 August 2026; **Published:** 9 September 2026

solid matrix deformation both contribute to the overall load-bearing capacity [1-7], and consequently influence frictional behaviour.

References [2-7] establish the same underlying mechanism—fluid pressurisation within a compressed, permeable, biological medium generating lift and reducing frictional resistance—in a sequence of related biomechanical contexts: lubrication theory for highly compressible porous media [2], the transfer of that theory to snow and skin contact [3, 4], and direct experimental measurement of lift generation inside compressible porous layers under both steady sliding and rapid compaction [5-7]. These studies are cited here because they collectively demonstrate that the same biphasic, pore-pressure-driven lift mechanism operates across a range of soft, permeable materials and loading regimes, providing the direct mechanistic precedent for applying this framework to engineered soft porous bearings in the present study.

Extensive research exists on rigid porous bearings and self-lubricating porous materials, and recent studies have identified key operating factors influencing their tribological performance, including critical porosity ranges [8], pore morphology [9], and lubricant supply mechanisms [10]. These investigations primarily concern porous materials with rigid or weakly deformable matrices and do not account for permeability changes arising from large elastic deformation. In soft porous bearings, permeability varies significantly with compression, fundamentally altering lubricant flow behaviour. This compressibility-driven variation in permeability leads to a different hydrodynamic lift generation mechanism and, consequently, a distinct friction response. Related theoretical work on squeeze-film and porous-plate lubrication with non-Newtonian and couple-stress fluids [21-26] further illustrates how strongly fluid rheology and slip conditions influence pressure generation in porous lubrication problems more broadly, reinforcing the case for treating fluid-phase behaviour explicitly rather than assuming a fixed, Newtonian, steady-state response. Despite its practical relevance, soft porous lubrication remains relatively new, and systematic investigations of its frictional performance are still limited.

A notable contribution to this field comes from the work of Zhu et al. [1], who examined how soft porous layers can reduce friction by conducting sliding experiments between a rigid flat slider and a compliant non-woven polyester surface. Their results showed that increasing the proportion of load carried by the fluid phase led to a corresponding reduction in the overall friction coefficient. The formula to calculate the proportion of load carried by the fluid phase is expressed as:

$$f_{air} = W_{fluid} / W_{total} \tag{1}$$

where W_{total} is the total load supported by the biphasic layer, and $W^{f}_{lui}{}^{d}$ is the load supported by the fluid phase.

To clarify how operating conditions influence friction reduction in soft porous lubrication, Zhu et al. [1] performed a systematic one-factor-at-a-time parametric study. They varied sliding speed, compression ratio (used as an analogue to angle of attack), initial precompression, slider length, and porous-layer stiffness. Their results showed that higher speeds, lower compression ratios, reduced precompression, longer contact lengths, and more compliant porous substrates all increased the fluid-phase load support fraction, f_{air}, which in turn lowered the friction coefficient μ. These trends highlight how strongly frictional behaviour in biphasic systems depends on both mechanical and geometric factors.

Under optimised conditions, Zhu et al. [1] achieved friction coefficients as low as $\mu = 0.04$, with the fluid phase carrying roughly 90% of the load. They further suggested that finer fibre networks, lower permeability materials, and higher-viscosity lubricants could enhance performance by improving fluid pressurisation and retention within the porous matrix.

However, while parametric studies help isolate the influence of individual variables, they do not fully capture the coupled interactions present in practical bearing systems. Many factors cannot be adjusted independently; for example, increasing sliding velocity naturally increases hydrodynamic pressurisation, which then changes the compression state of the porous layer—represented as precompression in planar tests or as eccentricity in journal bearings. Such interdependencies make it difficult to attribute friction trends to a single parameter.

Additionally, a key strength of soft porous lubrication—mirroring natural synovial joints—is its ability to provide both lubrication [1-7, 11, 12] and impact damping [13-15]. Constraining the porous layer's compression would suppress this adaptive response. Therefore, the current study focuses on friction behaviour under conditions where the compressed thickness of the porous material is free to evolve dynamically during operation.

This study aims to develop a practical method for evaluating material suitability and lubrication performance in soft porous lubrication systems under conditions that more accurately reflect the complex, interdependent variables present in real bearing environments, with a particular focus on how sliding speed, applied load, and lubricant viscosity govern friction under freely evolving compression. To achieve this, the Mini Traction Machine (MTM) was chosen as the primary test apparatus.

A major benefit of the MTM is that it allows the soft porous layer to compress and recover freely during operation, replicating the natural deformation seen in working bearings. This capability enables friction behaviour to be assessed without imposing artificial geometric constraints, thereby producing more representative performance data.

This work provides one of the first comprehensive assessments of soft porous materials tested under both dry and lubricated conditions, including a range of water-based lubricant formulations. By examining four foam-based materials and two woven fibrous substrates commonly considered for XPHD applications, the study offers new insight into how sliding speed, applied load, and lubricant viscosity govern friction in candidate media.

The principal novelty of this work is methodological as well as empirical: to the authors' knowledge, this is the first systematic experimental study of friction in soft porous lubrication that allows the porous layer's compression to evolve freely, rather than holding it fixed, across a matrix of six materials and five lubricant conditions. This departs from the fixed-compression protocols used in prior soft porous lubrication studies [1-7] and from the rigid-matrix assumptions underlying the existing porous-bearing literature [8-10], and it is this compression-free protocol that reveals the self-regulating friction behaviour reported in Sections 3 and 4.

2. Materials and Methods

The Mini Traction Machine (MTM) provides a controlled platform for measuring friction between contacting surfaces over a broad range of sliding speeds, applied loads, and lubrication conditions. For this study, the conventional MTM setup was modified to better suit the specific requirements of testing soft porous materials.

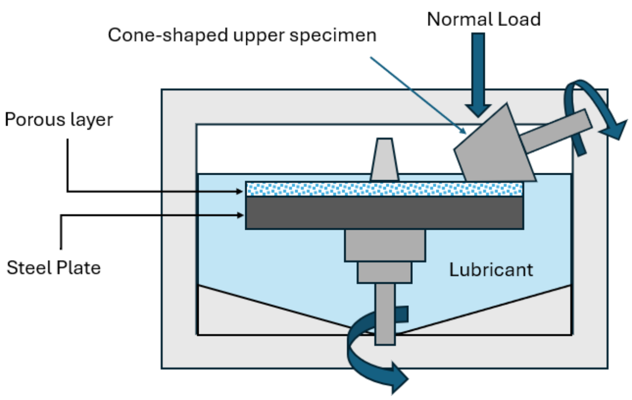

Figure 1. *Schematic of the MTM test set-up.*

In this modified MTM setup, the standard 3/4-inch steel ball was replaced with a custom cone-shaped upper specimen to create a broad, relatively flat contact region against the lower disc. The lower disc was machined to a smooth finish and fitted with interchangeable soft porous samples, ensuring stable alignment and consistent contact during testing (see Figure 1).

The cone geometry increased the contact width and spread the applied load over a larger area—an important requirement for compliant materials. Its elongated profile also reduced side-pressure leakage, a common issue in porous lubrication studies, by helping to confine the pressurised fluid within the contact zone. This confinement promoted the buildup of pore fluid pressure, thereby improving load-carrying capacity and reducing friction in fluid-saturated conditions. Overall, this configuration provided a more representative platform for assessing the behaviour of soft porous bearing materials.

All tests were conducted under controlled environmental conditions, with ambient temperature maintained at 25 ±2 ℃. The slide-roll ratio (SRR) was fixed at 200%, corresponding to pure sliding conditions. This configuration was selected to maximise the effect of soft porous lubrication, which works best during the sliding movements, due to the continuous convergence and divergence of the porous substrate.

To assess the frictional behaviour of soft porous materials under conditions representative of bearing operation, a tailored two-stage test protocol was developed for use with the modified MTM setup. This procedure was structured to capture the influence of both sliding velocity and normal load on friction performance. Each test consisted of two consecutive stages: in Stage 1 (variable speed at constant load), the normal load was fixed at 5 N while the sliding speed was incrementally increased from 5 mm/s to 120 mm/s, to characterise how friction responds to changes in sliding velocity; in Stage 2 (variable load at constant speed), the sliding speed was then held at 100 mm/s, and the normal load was gradually increased from 1 N to 7 N, to examine the effect of rising load—and therefore increasing compression of the porous layer—on friction.

In this manuscript, "friction coefficient" and "(adjusted) traction coefficient" are used interchangeably to refer to the same measured quantity, the ratio of tangential (friction) force to applied normal load. "Adjusted Traction Coefficient" is the native output field name reported by the MTM control software (PCS Instruments); "Adjusted" in this field name refers specifically to the software's rounding of the reported value to a fixed number of significant figures (three), rather than to any force-offset or baseline correction. "Traction coefficient" is retained in the figure axis labels because it is this software's native field name. Except where explicitly noted (Section 2.5, Equation (2)), the symbol μ denotes this friction/traction coefficient throughout; the distinct symbol η is used for lubricant dynamic viscosity to avoid ambiguity between the two.

For each material-lubricant pairing, measurements were repeated three times to ensure repeatability. The MTM automatically records friction force continuously, and its software calculates the instantaneous coefficient of friction. The mean value from the three repeated runs was used for analysis.

The same physical specimen was reused across Stage 1, Stage 2, and all three repeats for a given material-lubricant pairing, with a recovery interval allowed between runs. This is not expected to compromise the repeatability results in Table 2. First, the applied loads used in this study (1-7 N over the contact area) are low relative to the load range typically associated with permanent compression set in open-cell polyurethane foams and woven fibrous media; compression set predominantly develops under sustained, static loading, whereas the present tests apply dynamic, continuously sliding contact for a short duration per run. Second, the porous layer's recovery from compression is governed by fast, predominantly elastic cell-wall and fibre bending, not by slow diffusion-limited viscoelastic creep, so the bulk of the recovery is expected to occur within the recovery interval between runs, well before the next repeat began. During data inspection, the raw per-repeat values were examined in measurement order (repeat 1 → 2 → 3) for each test condition, and no systematic directional drift was observed; the scatter is consistent with random measurement variation rather than progressive compression set.

The lubrication mechanism investigated in this work is fundamentally different from classical hydrodynamic lubrication, as XPHD relies on the coupled interaction between pore-fluid pressurisation and large, reversible deformation of a compliant porous matrix. Because this mechanism is relatively new, no formal ASTM or ISO standards currently exist for friction testing of soft porous materials under dynamically varying compression, and standards developed for rigid contacts are not directly applicable. All friction experiments were conducted using a Mini Traction Machine (MTM) and followed the standard testing procedures inherent to the instrument, including constant slide-roll ratio tests with variable entrainment speed and constant-speed tests with variable load.

Six porous materials were selected for evaluation, representing two common categories of porous media. Two samples consisted of woven polyester fibrous structures, while the remaining four were open-cell polyurethane foams typically used in filtration and interface applications. The foam samples differed in both thickness and pore size, enabling comparison across a range of structural features. Table 1 summarises their physical properties, and Figures 2 to 6 provide corresponding surface-texture images. The porous layers were fixed to the lower plate using a combination of annular double-sided adhesive tape and glue. An annular strip of double-sided tape, cut to match the plate dimensions, was first applied to the plate, with a thin layer of glue added to reinforce adhesion. A second thin layer of glue was then applied to the exposed surface of the tape, and the porous material was carefully positioned on top to prevent edge lifting or in-plane sliding during testing.

This study is the first stage of a two-part investigation. Here, in Part 1, the six materials are treated as a single pool of candidate media and are named descriptively by the property most readily available for each type—nominal average pore size for the two open-pore foams (F450 and F280, denoting a nominal average pore diameter of 4.50 mm and 2.80 mm respectively, consistent with the measured pore-diameter ranges in Table 1) and nominal thickness for the remaining four (Foam 3 mm, Foam 5 mm, Woven 3.34, Woven 3.66). The naming is deliberately kept aligned with a companion paper (Part 2, in preparation), which isolates the effect of individual structural attributes—material type, pore dimensions, and thickness—by comparing matched pairs of materials that share every attribute except the one under study (e.g., Foam 3 mm vs. Foam 5 mm isolates thickness at fixed pore size; Woven 3.34 vs. Woven 3.66 isolates thickness at fixed weave; F450 vs. F280 isolates pore size at comparable thickness). Keeping the same material names across both papers allows the two studies to be read together without renaming or remapping specimens.

Pore diameter was measured from optical microscope images of the material surface (see Figures 2-6). Porosity was determined using the water saturation method: each specimen was weighed dry, then fully saturated with water and weighed again, and the volume of absorbed water (the mass difference divided by the density of water) was taken as the pore volume, from which porosity was calculated relative to the bulk volume of the dry specimen. For the woven materials, the surface is a mesh of interlaced fibres rather than an interconnected network of discrete pores, so a single pore-diameter value is not a meaningful descriptor of their structure; this is why Table 1 reports pore diameter as N/A for the two woven materials, while their porosity and thickness remain directly comparable to the foams.

All materials were tested under both dry and lubricated conditions. Lubricated tests employed water as the base fluid along with three additional formulations: 5% glycerol-water, 10% glycerol-water, and polyethylene glycol (PEG 400). These variants were chosen to examine how increased viscosity and friction-modifying characteristics affect soft porous lubrication performance. For reference, the dynamic viscosity of pure water is approximately 0.89 mPa s at 25 ℃, while PEG 400 is a substantially more viscous fluid, with reported dynamic viscosity in the range of approximately 90-130 mPa s at 20-25 ℃ [20], i.e. roughly two orders of magnitude higher than the glycerol solutions used here (≈ 1.2-1.35 mPa s, see Section 3.3). Despite this much higher viscosity, PEG 400 produced the lowest friction coefficients of any lubricant tested, which is consistent with its effect being dominated by boundary-lubrication and surface-coating chemistry rather than by viscous pore pressurisation alone (see Section 3.3). During lubricated tests, the fluid reservoir was fully submerged, ensuring continuous saturation of the porous layer throughout the experiment.

Table 1. *Characteristics of Porous Layers.*

Material name	Structure type	Pore diameter (mm)	Initial Porosity	Initial Thickness (mm)
F450	Open-pore foams	3.4-5.6	0.987	11.5
F280	Open-pore foams	2.2-3.4	0.982	10.5
Foam 3 mm	Open-pore foams	0.4-0.63	0.958	2.97

Material name	Structure type	Pore diameter (mm)	Initial Porosity	Initial Thickness (mm)
Foam 5 mm	Open-pore foams	0.4-0.63	0.958	4.82
Woven 3.34	Woven fibrous	N/A	0.968	3.34
Woven 3.66	Woven fibrous	N/A	0.976	3.66

Table 1 reports the properties needed to characterise and reproduce the six materials tested: pore diameter, porosity, and thickness. The foams and woven materials are generic, off-the-shelf products available from multiple commercial suppliers rather than a single proprietary formulation, so density and manufacturer/source add no further reproducibility value beyond these measured properties. Permeability is omitted for a different reason: it is not a fixed material constant in this system, but varies directly with the porous layer's compression state, the central variable under investigation here, so a single static value would misrepresent the material as behaving like a fixed-permeability medium. Stiffness is the exception — it plausibly contributes to the differing friction trends observed across materials under applied load (Section 3.2), and a compression-resolved mechanical characterisation, correlating compressive stress-strain behaviour with friction and lift performance, is the natural next step for this line of work.

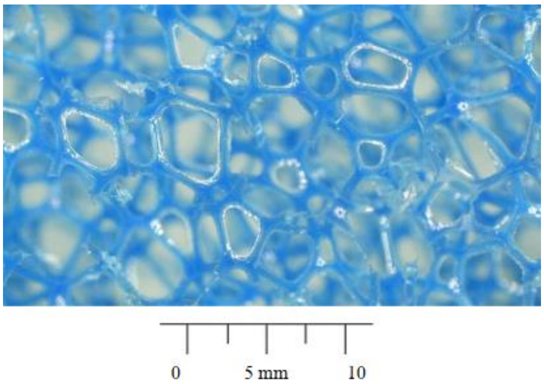

Figure 2. *F280 surface.*

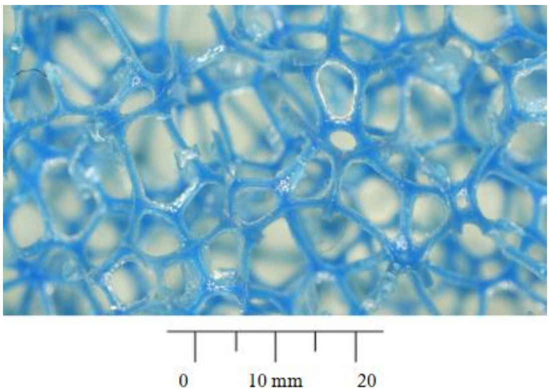

Figure 3. *F450 surface.*

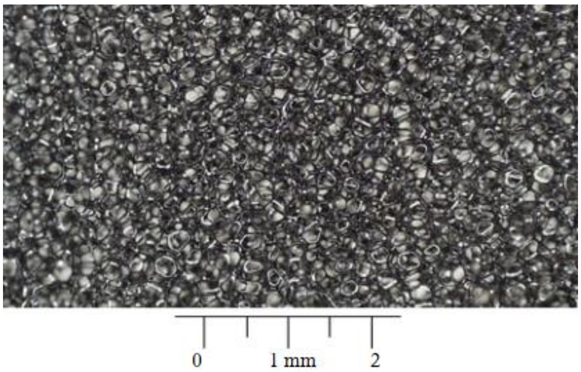

Figure 4. *Foam surface (same materials for 3 and 5 mm).*

Figure 5. *Woven 3.34 mm surface.*

Figure 6. *Woven 3.66 mm surface.*

2.1. Uncertainty Analysis

Experimental uncertainty was evaluated primarily through repeatability, supported by the manufacturer-calibrated control and measurement systems of the Mini Traction Machine (MTM, PCS Instruments). A summary of the identified sources of uncertainty is provided in Table 2. Repeated measurements enabled the calculation of mean values and standard deviations for the friction coefficient. For most porous material-lubricant combinations, the average percentage deviation in friction coefficient was typically within 10%, with the largest observed deviation not exceeding 21%. This level of variability demonstrates good repeatability for an experimental system involving compliant porous materials under dynamic deformation. Normal load, entrainment speed, and slide-roll ratio were controlled using the MTM's closed-loop systems, while friction force was measured using integrated calibrated transducers.

Table 2. *Uncertainty Analysis.*

Uncertainty source	Description	Treatment in this study
Normal load control	Closed-loop load control using manufacturer-calibrated MTM load system (PCS Instruments)	Load maintained constant throughout each test; repeatability assessed via repeated measurements
Speed and SRR control	Independent drive control of entrainment speed and slide-roll ratio (PCS Instruments)	MTM control software; consistency verified across repeated measurements
Friction force measurement	Calibrated force transducers integrated in the MTM (PCS Instruments)	Friction force continuously recorded; variability captured through repeat measuring
Data processing	Averaging and signal filtering	Effect minimised through consistent processing procedures
Test repeatability	Variability between repeated tests under identical conditions	For each test condition, three repeated measurements were performed, and uncertainty was quantified using the standard deviation; the average percentage deviation across all test conditions ranged from approximately 4% to 21%.

2.2. Theoretical Framework

In the experimental work of Zhu et al. [1], it was demonstrated that the contribution of the fluid phase, specifically the generation of pore pressure, plays a significant role in determining the frictional behaviour of soft porous lubrication systems. The underlying principle is that increasing the fluid phase contribution while reducing the proportion of load carried by the solid matrix results in a lower overall friction coefficient. Under fixed compression conditions, where both pre-compression and operating compression remain constant throughout testing, this relationship can be described and predicted using steady-state theoretical models. For example, the generated pressure underneath the planar board can be expressed using Pascovici's [12] theoretical model:

$$p = \frac{\eta u L}{D}\frac{(1-\emptyset_0)(1-\emptyset_2)}{(1-\emptyset^*)(\emptyset_0-\emptyset_2)}\left(\frac{1}{\emptyset}-\frac{\emptyset^*}{2\emptyset^2}+c\right) \quad (2)$$

where p is the pressure, η is the lubricant dynamic viscosity, u is the sliding velocity, L is the contact length in the sliding direction, D is the thickness of the porous layer, $\emptyset_0$ and $\emptyset_2$ are the porosities at the leading and trailing edges of the slider, c $= \emptyset^*/2\emptyset_0^2 - 1/\emptyset_0$, and $\emptyset^* = 2\emptyset_0\emptyset_2 / (\emptyset_0 + \emptyset_2)$ is the porosity at the point of maximum pressure [11].

Equation (2) is a steady-state, fixed-compression model and is used here only as the theoretical point of comparison against which the present, dynamically-compressed results are contrasted in Section 4. Neither pore pressure nor instantaneous layer compression was measured directly in this study; the self-regulating feedback loop proposed in Section 4 to explain the observed friction trends is therefore an inference drawn from the friction data, not a directly measured mechanism. Direct measurement of pore pressure and compression is identified as a priority for future work (see Conclusions).

3. Results

Figures 7-18 plot error bars on every data point, representing ± one standard deviation across the three repeated measurements for that test condition. This provides a direct visual indication of measurement scatter alongside the quantified repeatability summary in Table 2 (Section 2.4) and the percentage-deviation annotations in Figure 18, which together range from approximately 4% to 21% depending on test condition. Descriptive terms used below such as “marginally,” “largely stable,” and “plateau” refer to changes that are small relative to this error-bar range rather than to a formal statistical significance test; where two conditions' error bars overlap substantially, the corresponding trend should be read with correspondingly less confidence.

Part (a) of Figures 7-12 illustrates the relationship between the measured friction coefficient and sliding velocity for the tested materials, while part (b) shows the corresponding dependence on normal load. For the polyurethane foams, the frictional behaviour is presented in Figures 7-10, whereas the woven porous materials are shown in Figures 11 and 12. In addition, to aid the comparison, Figures 13-17 compare the porous layer performance for each working fluid and lubrication mode.

In each panel of Figures 7-12, the ‘Dry’ curve sits well above the four lubricated conditions, which compresses Water, Gly5, Gly10 and PEG into a narrow band close to the x-axis where the curves frequently cross. The absolute gap between Dry and any lubricated condition is the main point of those four clustered curves; the relative ranking between Water, Gly5, Gly10 and PEG is the focus of Section 3.3 and is easier to read from the consolidated heatmap (Figure 18), which reports the average value and percentage deviation for every material-lubricant combination directly.

3.1. Effect of Sliding Speed

The variation of the friction coefficient with sliding speed was analysed using part (a) of Figures 7 to 12. Insights into the interaction between compression and pore-pressure generation can be drawn from the first stage of testing, in which speed was varied while the normal load remained constant. In literature, under steady-state conditions, higher sliding velocities would generally be expected to increase fluid pressurisation and raise the fluid-phase load support, as indicated by Equation (2) in Section 2.5. This should reduce friction—a trend also reported by Zhu et al. [1], whose tests maintained a fixed compression level.

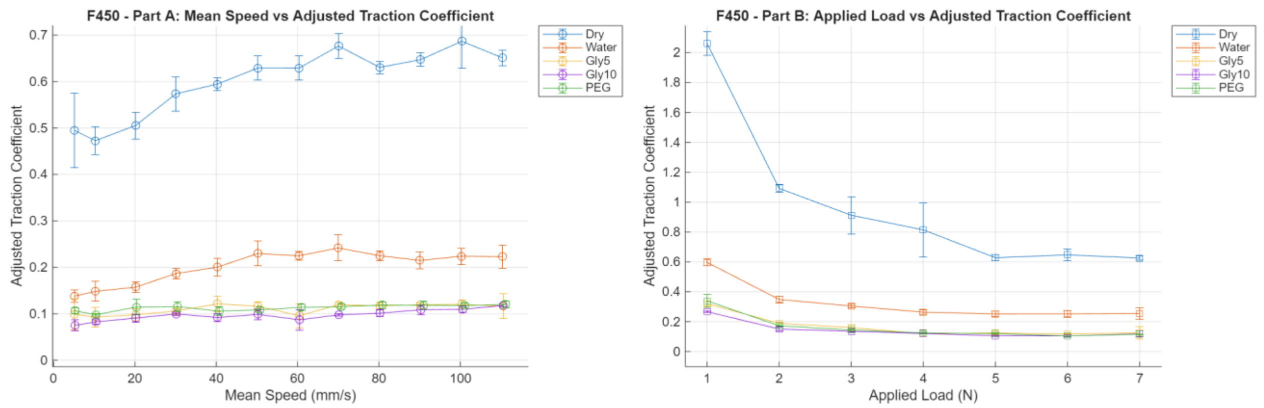

(a) (b)

Figure 7. Friction coefficient plot for material F450: (a) Mean Speed vs Adjusted Traction Coefficient; (b) Applied Load vs Adjusted Traction Coefficient.

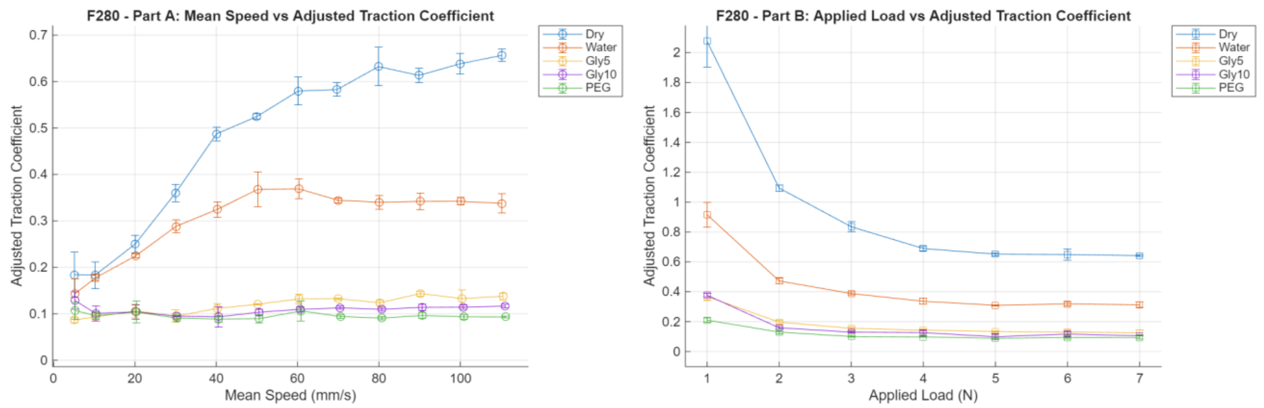

(a) (b)

Figure 8. Friction coefficient plot for material F280: (a) Mean Speed vs Adjusted Traction Coefficient; (b) Applied Load vs Adjusted Traction Coefficient.

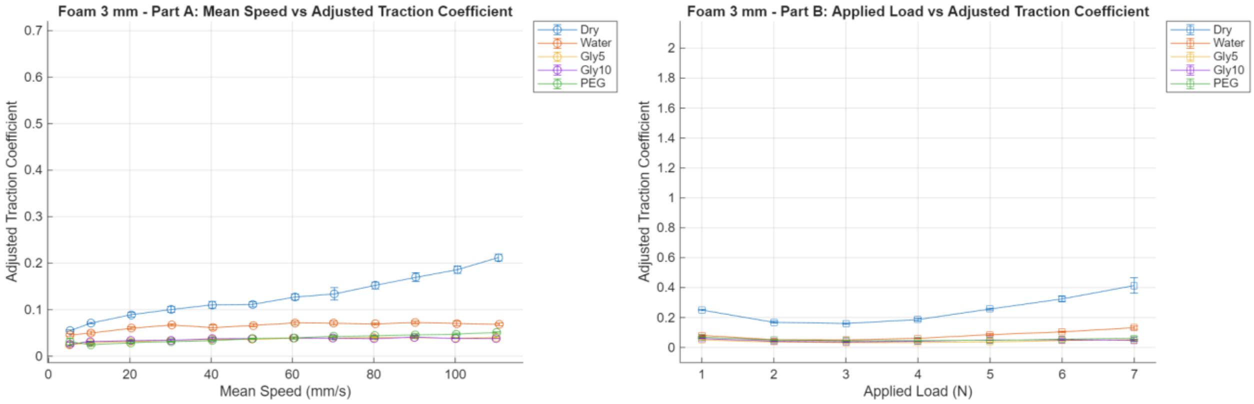

(a) (b)

***Figure 9**. Friction coefficient plot for material Foam 3 mm: (a) Mean Speed vs Adjusted Traction Coefficient; (b) Applied Load vs Adjusted Traction Coefficient.*

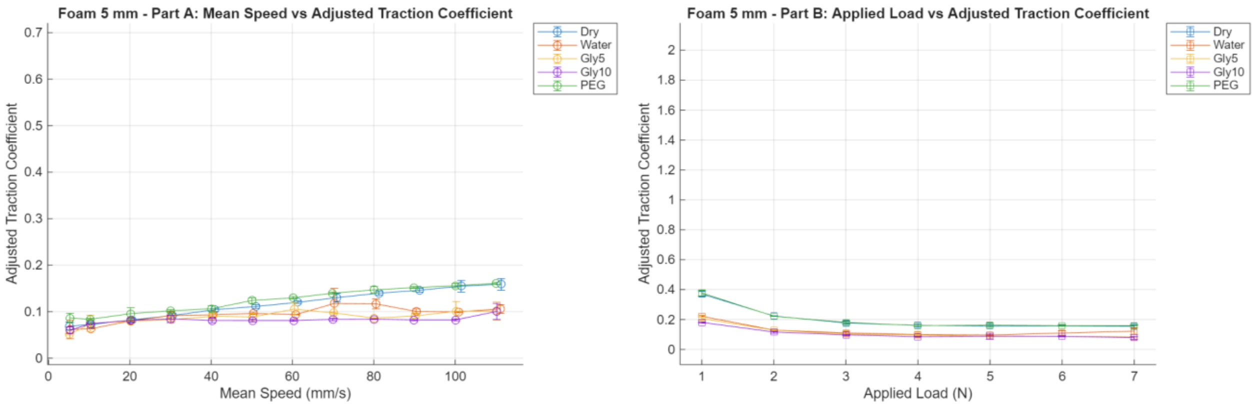

(a) (b)

***Figure 10**. Friction coefficient plot for material Foam 5 mm: (a) Mean Speed vs Adjusted Traction Coefficient; (b) Applied Load vs Adjusted Traction Coefficient.*

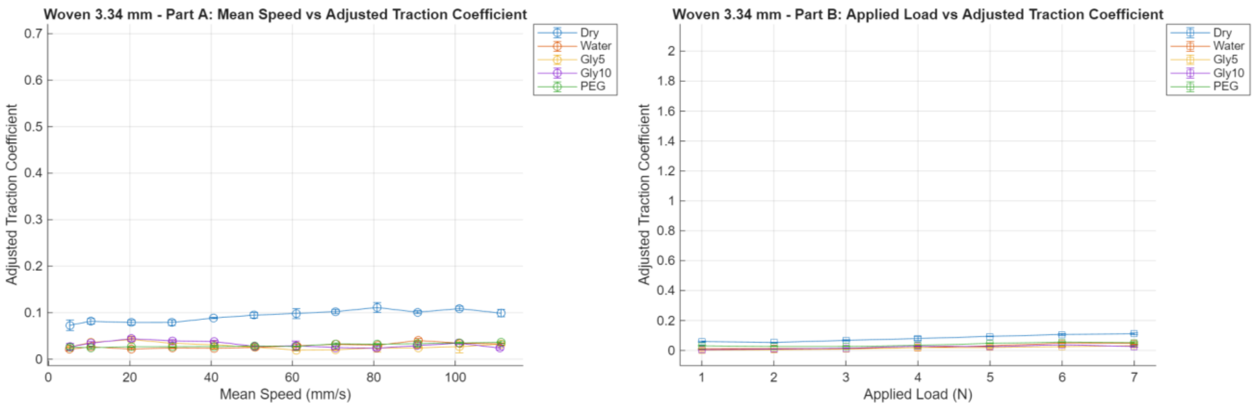

(a) (b)

***Figure 11**. Friction coefficient plot for material Woven 3.34 mm: (a) Mean Speed vs Adjusted Traction Coefficient; (b) Applied Load vs Adjusted Traction Coefficient.*

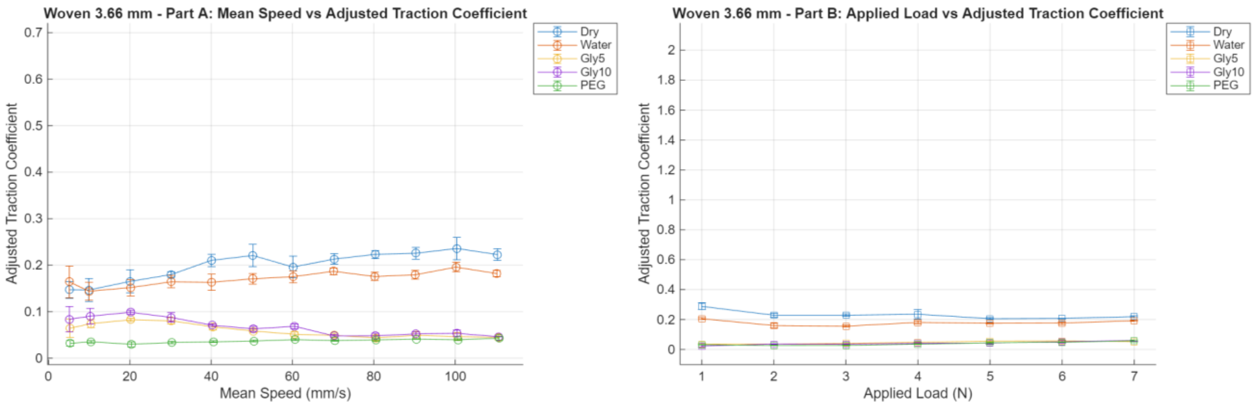

(a) (b)

Figure 12. *Friction coefficient plot for material Woven 3.66 mm: (a) Mean Speed vs Adjusted Traction Coefficient; (b) Applied Load vs Adjusted Traction Coefficient.*

In the present study, however, this behaviour did not consistently occur. For all foam-based materials (part (a), Figures 7-10), the friction coefficient either changed very little or increased as speed rose, regardless of the lubricant used. These results imply that any increase in pore pressure was offset by lift-induced reductions in compression, preventing additional friction reduction. It appears that friction was dominated by the solid-phase component of the porous medium, which is largely insensitive to pressure changes, thereby keeping the overall friction coefficient nearly constant.

The woven fibrous materials (Figures 11 and 12) showed a different response, especially when glycerol-containing lubricants were used. A slight decrease in friction was observed at lower speeds, but the effect levelled off as velocity increased. This again indicates a dynamic equilibrium among pore-pressure generation, material deformation, and lift.

Overall, the results highlight the importance of allowing the porous layer to compress freely when assessing soft porous lubrication. They also demonstrate that frictional trends under dynamic, deformable conditions may differ markedly from predictions based on fixed-compression models—particularly in systems where the porous medium can adjust its thickness in response to operating loads.

3.2. Effect of Applied Load

The results show that, in contrast to the behaviour predicted for fixed-compression systems, increasing applied load does not consistently result in increased friction coefficient. For the majority of the materials tested, the friction coefficient remained within the range of measurement uncertainty established in Table 2 (typically ≤10% deviation) as the load was increased from 1 N to 7 N, as can be seen in part (b) of Figures 7-12—that is, these changes are not resolvable from repeatability scatter alone, rather than being a precisely constant value. This suggests that the system dynamically balances the increase in load with corresponding adjustments in pore pressure and compression, effectively maintaining stable friction performance within this load range.

An exception to this trend was observed with the thinner woven fibrous material and the 3 mm foam material, which exhibited an increase in friction as the load increased. However, it is important to note that these materials still demonstrated the lowest overall friction coefficients among all specimens tested.

These findings further reinforce that the friction behaviour of soft porous lubrication systems with variable compression cannot be fully explained by steady-state or fixed-compression models.

Differences in friction response between materials under increasing load are likely influenced by variations in porous-layer stiffness, which affects compression behaviour and, in turn, pore-pressure generation. A compression-resolved mechanical characterisation, correlating compressive stress-strain behaviour with friction and lift performance, is the natural next step for this line of work (see Table 1).

3.3. Effect of Fluid Viscosity

Across nearly all materials, the introduction of a liquid lubricant markedly reduced friction compared with dry (air) conditions, as highlighted in the consolidated summary plots (Figures 13-17). This difference is attributable to air's much lower viscosity and correspondingly different fluid-transport characteristics relative to the tested liquids: as indicated by Equation (2) in Section 2.5, generated pressure scales directly with fluid viscosity, so air's viscosity (≈ 0.018 mPa·s at 25 ℃, roughly four orders of magnitude below water) is far too low to build meaningful pore pressure or lift within the porous layer under the tested sliding speeds, leaving the solid matrix to carry most of the load and limiting the effectiveness of soft porous lubrication. Using water, with its higher viscosity, produced a clear reduction in friction by enhancing fluid pressurisation and surface separation.

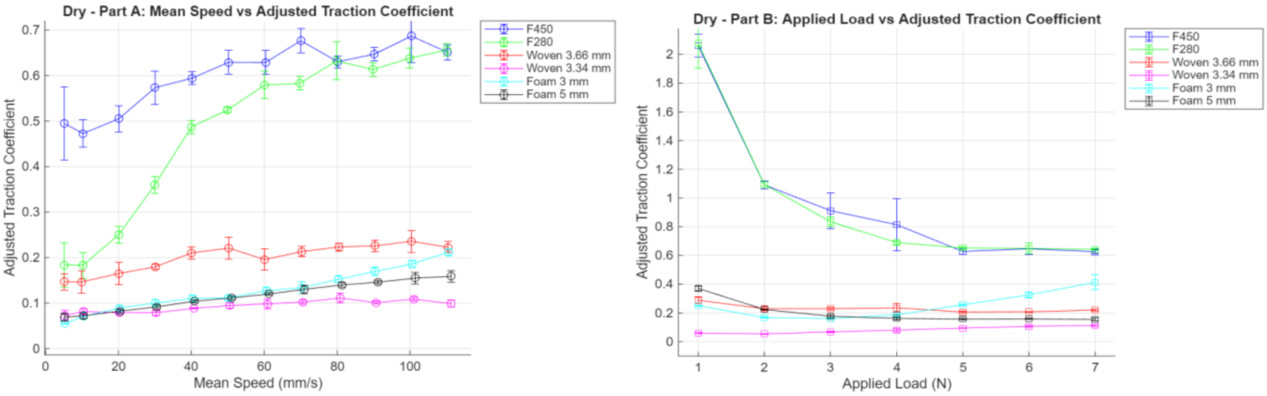

(a) (b)

Figure 13. *Friction coefficient plot for dry condition: (a) Mean Speed vs Adjusted Traction Coefficient; (b) Applied Load vs Adjusted Traction Coefficient.*

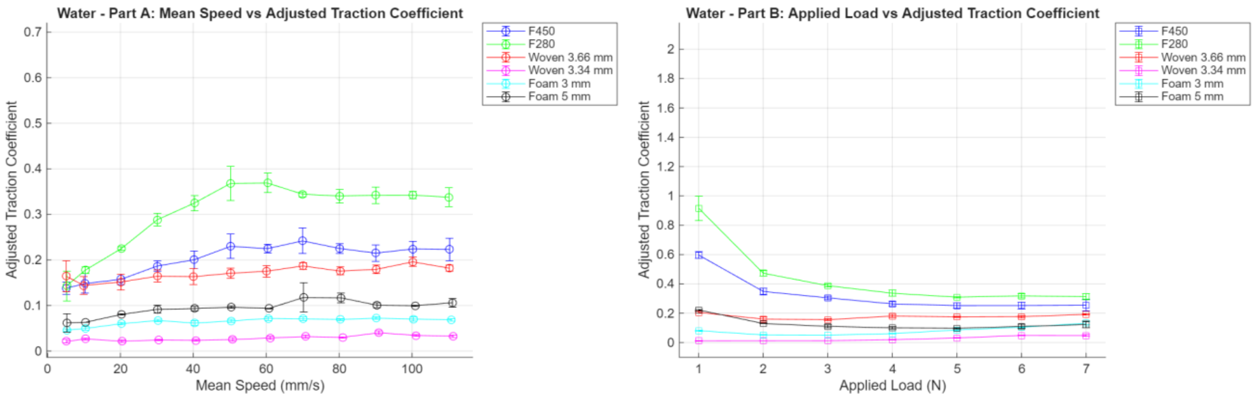

(a) (b)

Figure 14. *Friction coefficient plot for water lubricated condition: (a) Mean Speed vs Adjusted Traction Coefficient; (b) Applied Load vs Adjusted Traction Coefficient.*

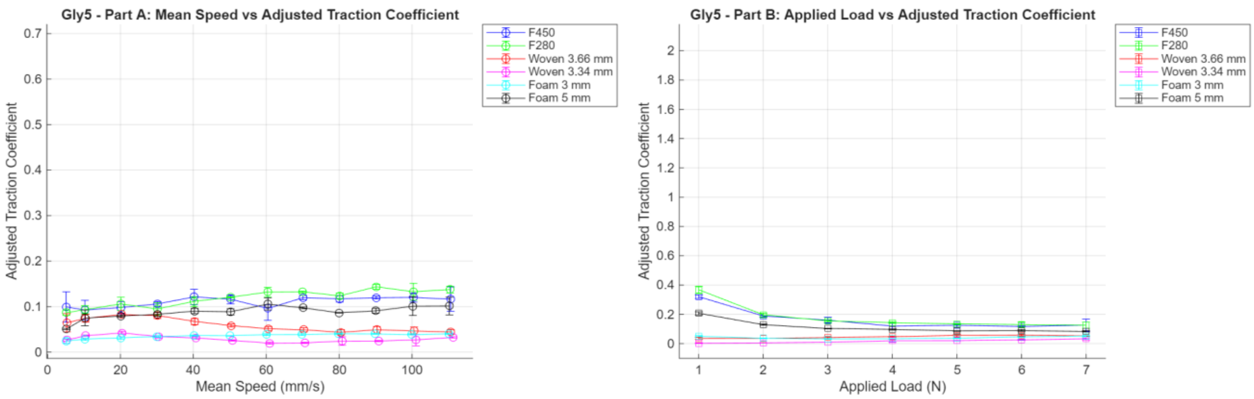

(a) (b)

Figure 15. *Friction coefficient plot for glycerol 5% lubricated condition: (a) Mean Speed vs Adjusted Traction Coefficient; (b) Applied Load vs Adjusted Traction Coefficient.*

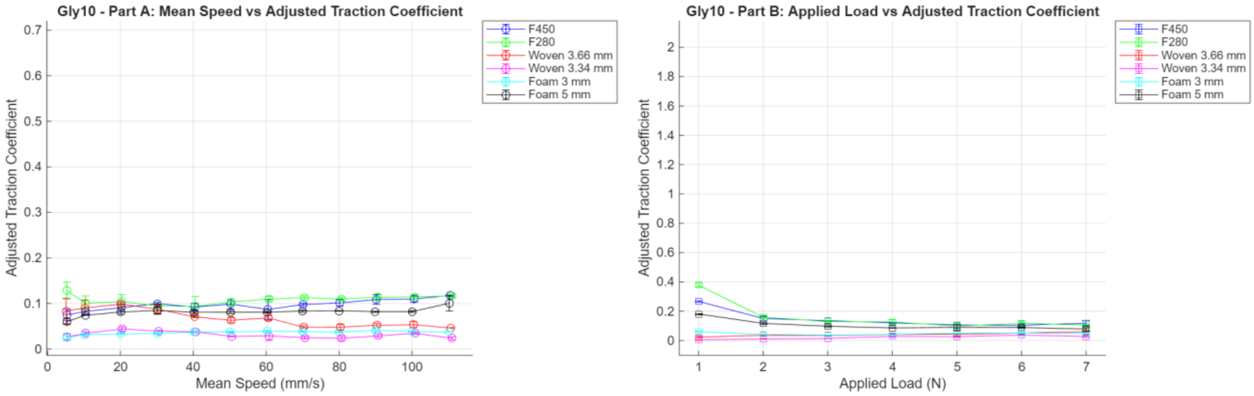

(a) (b)

Figure 16. *Friction coefficient plot for glycerol 10% lubricated condition: (a) Mean Speed vs Adjusted Traction Coefficient; (b) Applied Load vs Adjusted Traction Coefficient.*

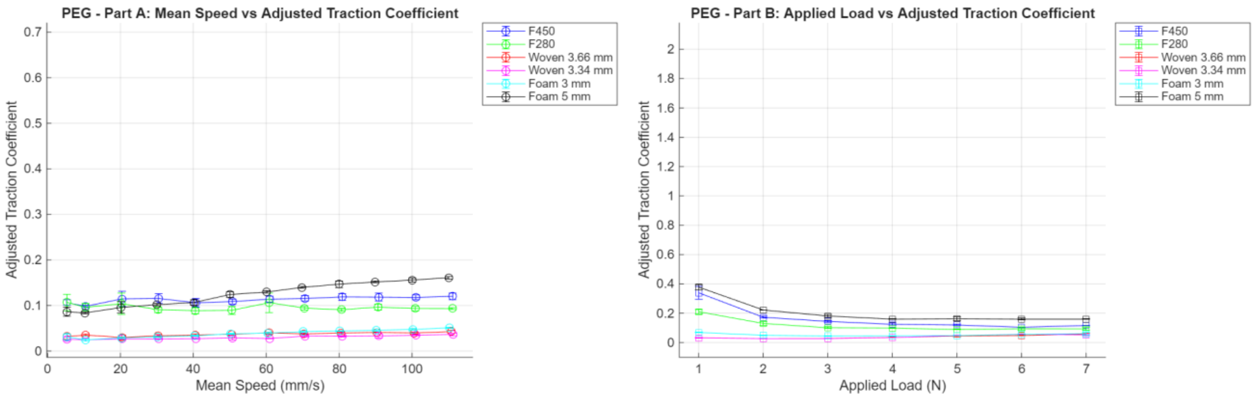

(a) (b)

Figure 17. *Friction coefficient plot for PEG 400 lubricated condition: (a) Mean Speed vs Adjusted Traction Coefficient; (b) Applied Load vs Adjusted Traction Coefficient.*

A further improvement was observed with the 5% glycerol solution (η ≈ 1.2 mPa·s at 23-25 ℃, as reported by Segur and Oberstar [16]). Its slightly higher viscosity promoted increased lift pressure generated by the fluid phase, and this improvement was substantial rather than marginal: averaged across the six materials, the transition from water to 5% glycerol reduced the mean adjusted traction coefficient by approximately 37% (Figure 18(a); individual materials ranged from a 7% to a 65% reduction). Increasing the concentration to 10% (η ≈ 1.3-1.35 mPa s at 23-25 ℃ [16]), by contrast, produced a mean change of less than 1% across the same six materials and was not consistently a further reduction: two materials (Foam 3 mm, Woven 3.66 mm) showed a small increase rather than a continued decrease. This asymmetry — a large, consistent benefit from introducing glycerol, followed by a negligible and inconsistent effect of doubling its concentration — is the basis for describing the viscosity benefit as plateauing beyond 5%. This apparent plateau is interpreted phenomenologically and may be associated with a hypothesised glycerol-related surface-coating effect; once the porous solid matrix is sufficiently wetted and smoothed by the lubricant, further increases in viscosity are inferred to have a diminishing influence on fluid-solid interactions. This behaviour also reflects the self-regulating nature of XPHD systems—greater viscosity increases pore pressure, but the resulting lift reduces compression, limiting further gains in fluid-phase support.

Polyethylene glycol (PEG 400) was included as a synthetic analogue to friction-modifying components found in synovial fluid (e.g., lubricin, albumin) [17-19]. PEG consistently produced the lowest friction values, particularly in the woven polyester materials (Figure 17(a)), where the minimum instantaneous friction coefficient observed across the speed sweep dropped to 0.05 for the 3.66 mm specimen and 0.02 for the 3.34 mm specimen; these are single-point minima read directly from the curves in Figure 17(a), and are lower than the corresponding average values reported in Figure 18 (0.037 and 0.030 respectively), which average over the full speed range rather than reporting the best-case point. PEG also significantly reduced friction in several foam samples, with the strongest effect observed in the 3 mm foam.

The 5 mm foam, however, showed minimal sensitivity to

PEG despite being made of the same base material. The thicker foam undergoes greater deformation, causing sliding to occur through a thicker, more viscous PEG-filled region and requiring longer fluid flow paths. These effects increase viscous resistance and counteract part of the lubrication benefit. In the thinner 3 mm foam, this viscous penalty is much smaller, allowing PEG's boundary-lubrication advantages to dominate.

Figure 18 summarises these trends as a consolidated heatmap of the average adjusted traction coefficient for every material-lubricant combination, extracted from both the variable-speed (part (a)) and variable-load (part (b)) tests, with the percentage deviation across repeated measurements shown in parentheses. Lighter regions correspond to higher friction, whereas darker regions indicate better lubrication performance; this view makes the ranking between Water, Gly5, Gly10 and PEG immediately readable without relying on the individual curves above.

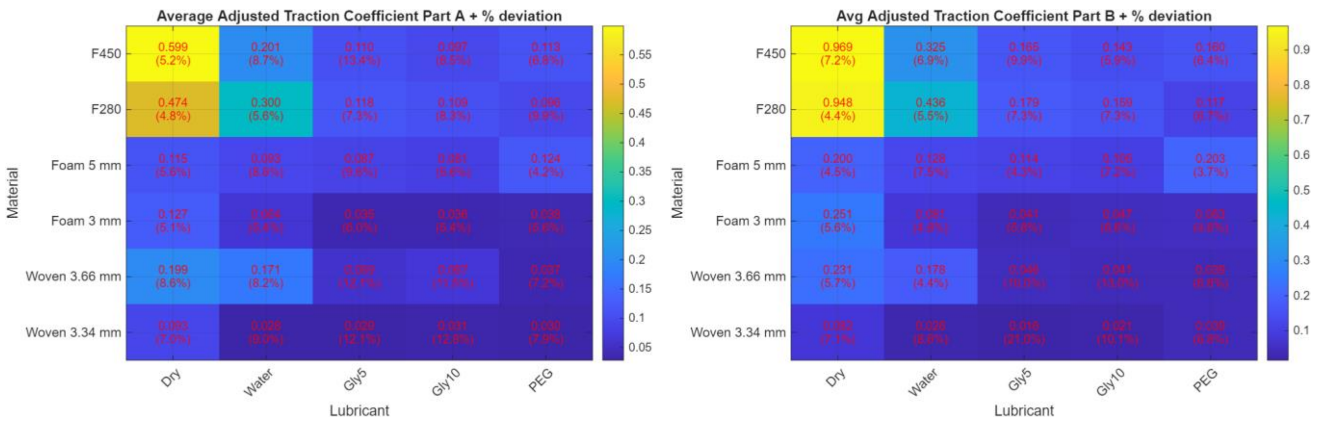

(a) (b)

Figure 18. Average friction coefficient map (with percentage deviation) for: (a) Mean Speed vs Adjusted Traction Coefficient; (b) Applied Load vs Adjusted Traction Coefficient.

4. Discussion

In contrast, the present study was designed to allow the compression of the porous layer to vary dynamically during operation, to better reflect the conditions that would be present in an actual bearing. Under such conditions, the interaction between compression and pore pressure becomes more complex. As the porous layer compresses, pore pressure increases; however, the resulting increase in fluid lift acts to reduce compression, thereby moderating the further buildup of pressure. This creates a self-regulating feedback loop in which both the compression state and the fluid-phase load support continuously adjust in response to one another. Consequently, the resulting friction behaviour cannot be fully captured by models developed for steady-state, fixed-compression conditions [1, 2, 12].

This self-regulating mechanism accounts for the results reported above: the near-constant or increasing friction with sliding speed (Section 3.1), the load-independence of friction across most materials (Section 3.2), and the plateauing benefit of increasing lubricant viscosity beyond 5% glycerol (Section 3.3) are all consistent with a system in which any gain in pore pressure is continuously offset by a corresponding reduction in compression, rather than with the monotonic trends predicted by Equation (2) under fixed compression.

A quantitative, point-by-point fit of the present data against Equation (2) was deliberately not attempted, and this is a direct consequence of the compression-free protocol rather than a gap to be filled with additional analysis. Equation (2) is derived for a fixed compression state: it assumes a constant porosity distribution (through $\varnothing_0$, $\varnothing_2$ and $\varnothing^*$) and a fixed layer thickness D, both held constant while pressure is evaluated. In the present tests, however, compression is free to evolve continuously with sliding speed and load, so the porosity distribution and effective layer thickness that Equation (2) treats as fixed inputs are themselves changing, unmeasured, outputs of the system at every instant. Fitting the fixed-compression model to variable-compression data would therefore require assuming a porosity/thickness state that the experiment was specifically designed not to hold constant, which would not test the model on its own terms and could misrepresent the comparison as more quantitative than the underlying assumptions support. For this reason, Equation (2) is used here only qualitatively, as the fixed-compression reference point against which the observed trends are contrasted, and a genuine quantitative comparison would require a fixed-compression variant of the same protocol — or direct, time-resolved measurement of compression and pore pressure — which we identify as necessary future work (see Conclusions) rather than attempt here.

Taken together, these results indicate that the frictional performance of soft porous lubrication is governed less by any single operating parameter than by the coupled evolution of pore pressure and layer compression. This has practical implications for bearing design: selecting lubricant viscosity and operating conditions requires accounting for how the compression state evolves during operation, rather than relying solely on steady-state predictions such as Equation (2). More broadly, the results reinforce the case made in the Introduction—drawing on the analogy with synovial joints—that constraining the compression of a soft porous layer, whether in test rigs or in theoretical models, removes exactly the adaptive response that gives this lubrication mechanism its practical advantage.

5. Conclusions

This study explored the influence of sliding speed, applied load, and lubricant viscosity on the friction performance of soft porous materials under dynamically evolving compression. Key findings include:

1) Variable compression significantly influences friction trends, overriding predictions from steady-state models.
2) Sliding speed and load do not consistently reduce or increase friction, due to the self-regulating interaction between pore pressure and compression.
3) Fluid viscosity improves lubrication up to a point, beyond which further viscosity increases offer diminishing returns.

These insights highlight the need for dynamic testing approaches when evaluating soft porous lubrication systems and will benefit the selection of lubricant formulations and operating conditions for advanced low-friction, long-life bearings.

It should be noted that “long-life bearing designs” above refers to the motivating application for this line of research rather than to a claim evaluated in this study: wear progression and long-term durability were outside the scope of the present work, which examined only friction under short-duration test protocols. Assessing wear and durability directly is identified as necessary future work before the findings here can support specific bearing-life claims.

Soft porous lubrication remains a relatively new and emerging research topic, and the present work represents one of the first experimental studies to systematically examine friction behaviour under dynamically deformable, load-controlled conditions. While this study establishes a baseline experimental framework and identifies key trends, further work is required to quantify material properties such as permeability, compressive behaviour, evolving contact conditions, material degradation and surface evolution, as well as to incorporate direct measurements of deformation and fluid transport. Such investigations will be essential for developing predictive models and translating XPHD lubrication concepts into practical bearing applications.

Abbreviations

MTM	Mini Traction Machine
XPHD	Ex-Poro-HydroDynamic
SRR	Slide-Roll Ratio
PEG	Polyethylene Glycol

Acknowledgments

The author would like to thank Tung Tran for the assistance in proofreading the manuscript.

Author Contributions

Duc Hieu Nguyen: Conceptualization, Formal Analysis, Investigation, Methodology, Writing – original draft, Writing – review & editing

Data Availability Statement

The data that support the findings of this study are available from the corresponding author upon reasonable request.

Conflicts of Interest

The author declares no conflict of interest.

References

[1] Zhu, Z., Weinbaum, S., Wu, Q. Experimental Study of Soft Porous Lubrication. Physical Review Fluids. 2019, 4, 024305. https://doi.org/10.1103/PhysRevFluids.4.024305

[2] Feng, J., Weinbaum, S. Lubrication Theory in Highly Compressible Porous Media: The Mechanics of Skiing, from Red Cells to Humans. Journal of Fluid Mechanics. 2000, 422, 281-317. https://doi.org/10.1017/S0022112000001725

[3] Wu, Q., Igci, Y., Andrepoulos, Y., Weinbaum, S. From Red Cells to Snowboarding: A New Concept for a Train Track. Physical Review Letters. 2004, 93, 194501. https://doi.org/10.1103/PhysRevLett.93.194501

[4] Wu, Q., Igci, Y., Andrepoulos, Y., Weinbaum, S. Lift Mechanics of Downhill Skiing and Snowboarding. Medicine & Science in Sports & Exercise. 2006, 38, 1132-1146. https://doi.org/10.1249/01.mss.0000222842.04510.83

[5] Gacka, T., Zhu, Z., Crawford, R., et al. From Red Cells to Soft Lubrication: An Experimental Study of Lift Generation inside a Compressible Porous Layer. Journal of Fluid Mechanics. 2017, 818, 5-25. https://doi.org/10.1017/jfm.2017.133

[6] Zhu, Z., Nathan, R., Wu, Q. An Experimental Study of the Lubrication Theory for Highly Compressible Porous Media, with and without Lateral Leakage. Tribology International. 2018, 127, 324-332. https://doi.org/10.1016/j.triboint.2018.06.016

[7] Zhu, Z., Nathan, R., Wu, Q. Multi-Scale Soft Porous Lubrication. Tribology International. 2019, 137, 246-253. https://doi.org/10.1016/j.triboint.2019.05.003

[8] Xu, X., Shu, X. W., Pei, Q., Qin, H. L., Guo, R., Wang, X. L., Wang, Q. H. Effects of Porosity on the Tribological and Mechanical Properties of Oil-Impregnated Polyimide. Tribology International. 2022, 170, 107502. https://doi.org/10.1016/j.triboint.2022.107502

[9] Ye, J., Li, J., Qing, T., Huang, H., Zhou, N. Effects of Surface Pore Size on the Tribological Properties of Oil-Impregnated Porous Polyimide Material. Wear. 2021, 484-485, 204042. https://doi.org/10.1016/j.wear.2021.204042

[10] Chen, W., Wang, C., Zhou, G., Liu, F., Wang, W., Zhu, P. Molecular Dynamics Simulations of Lubricant Supply in Porous Polyimide Bearing Retainers. Lubricants. 2024, 12, 343. https://doi.org/10.3390/lubricants12100343

[11] Nguyen, D. H., Herzig, N., Glovnea, R. Pressure Evaluation in Highly Porous Medium Hydrodynamic Bearings. Proceedings of the Institution of Mechanical Engineers, Part J: Journal of Engineering Tribology. 2024, 238(5). https://doi.org/10.1177/13506501241253879

[12] Pascovici, M. D. Lubrication Processes in Highly Compressible, Porous Layers. In Proceedings of Lubrification et Tribologie des Revêtements Minces, Poitiers, France, 22-23 May 2007.

[13] Pascovici, M. D., Popescu, C. S., Marian, V. G. Impact of a Rigid Sphere on a Highly Compressible Porous Layer Imbibed with a Newtonian Liquid. Proceedings of the Institution of Mechanical Engineers, Part J: Journal of Engineering Tribology. 2010, 224, 789-795. https://doi.org/10.1243/13506501JET775

[14] Ilie, M.-B., Pascovici, M. D., Marian, V. G. Squeeze Processes in a Narrow Circular Damper with Highly Compressible Porous Layer Imbibed with Liquids. Proceedings of the Institution of Mechanical Engineers, Part J: Journal of Engineering Tribology. 2011, 225, 539-549. https://doi.org/10.1177/1350650111399992

[15] Crawford, R., Nathan, R., Wang, L., Wu, Q. Experimental Study on the Lift Generation inside a Random Synthetic Porous Layer under Rapid Compaction. Experimental Thermal and Fluid Science. 2012, 36, 205-216. https://doi.org/10.1016/j.expthermflusci.2011.09.014

[16] Segur, J. B., Oberstar, H. E. Viscosity of Glycerol and Its Aqueous Solutions. Industrial & Engineering Chemistry. 1952, 44, 2117-2120. https://doi.org/10.1021/ie50501a040

[17] Heuberger, A., et al. Conformational and Adsorptive Characteristics of Albumin Affect Interfacial Protein Boundary Lubrication: From Experimental to Molecular Dynamics Simulation Approaches. Colloids and Surfaces B: Biointerfaces. 2009, 68, 171-177.

[18] Hills, B. A. Boundary Lubrication in Vivo. Proceedings of the Institution of Mechanical Engineers, Part H: Journal of Engineering in Medicine. 2000, 214, 83-94. https://doi.org/10.1243/0954411001535301

[19] Jay, G. D., Waller, K. A. The Biology of Lubricin: Near Frictionless Joint Motion. Matrix Biology. 2014, 39, 17-24. https://doi.org/10.1016/j.matbio.2014.08.008

[20] Altalbawy, F., Al-Hussainy, A., Doshi, H., Ganesan, S., Agarwal, M., Kaur, P., Saydaxmetova, S., Nafea, M., Najm, M., Al-Shami, K., Kiani, M. Dynamic Viscosity of Polyethylene Glycol (PEG): Data Assessment, Sensitivity Analysis and Robust Modeling via Artificial Intelligence Methods. Polymers for Advanced Technologies. 2024, 35, e6596. https://doi.org/10.1002/pat.6596

[21] Devani, U., Patil, J., Bilal, S., Hanumagowda, B. N., Trimbak, V. B., Tawade, J. V., Nazarova, N., Gupta, M. Study of MHD on Porous Flat and Curved Circular Plate Lubricated with Couple Stress Fluid — A Slip Velocity Model. Results in Engineering. 2024, 24, 102914. https://doi.org/10.1016/j.rineng.2024.102914

[22] Dandoti, S. M., Ali, A. B. M., Patil, J., et al. Squeeze Film Performance on Curved Circular and Flat Plate with Magnetic Field and Slip-Velocity with Non-Newtonian Fluid. Journal of Vibration Engineering & Technologies. 2025, 13, 495. https://doi.org/10.1007/s42417-025-02005-2

[23] Devani, U., Patil, J., Hanumagowda, B. N., Tawade, J. V., Kulkarni, N. V. MHD Slip and Surface Roughness Effects in Fluid-Based Hydrodynamic Lubrication of Secant Curved Circular Plates. Proceedings of the Institution of Mechanical Engineers, Part N: Journal of Nanomaterials, Nanoengineering and Nanosystems. 2026, OnlineFirst. https://doi.org/10.1177/23977914261429788

[24] Kempepatil, R., Hiremath, A. G., Hanumagowda, B. N., Patil, J., Tawade, J. V., Khan, M. I. Influence of Magneto-Hydrodynamic and Couple Stress Squeeze Film Lubrication on Conical Bearing — A Slip Velocity Model. Alexandria Engineering Journal. 2024, 106, 735-742. https://doi.org/10.1016/j.aej.2024.08.064

[25] Devani, U., Patil, J., Hanumagowda, B. N., Hejazi, H. A., Patil, V., Tawade, J. V., Elkamchouchi, D. H., Ali, S. Features of MHD Slip Velocity on Secant Curved Porous Circular Plates with Couple-Stress Fluid. International Communications in Heat and Mass Transfer. 2025. https://www.sciencedirect.com/science/article/abs/pii/S0735193325012497

[26] Vijayalaxmi, Patil, J., Hanumagowda, B. N., Tawade, J. V., Khan, M. I. Performance of Surface Roughness of MHD Slip Velocity on Curved Circular and Flat Plates Lubricated with Non-Newtonian Fluid. International Journal of Hydrogen Energy. 2024, 87, 1522-1532. https://doi.org/10.1016/j.ijhydene.2024.08.500